© 2015. Published by The Company of Biologists Ltd | The Journal of Experimental Biology (2015) 218, 184-193 doi:10.1242/jeb.111187

RESEARCH ARTICLE

Bird colour vision: behavioural thresholds reveal receptor noise

Peter Olsson[1,*], Olle Lind[1,2,3] and Almut Kelber[1]

ABSTRACT

Birds have impressive physiological adaptations for colour vision, including tetrachromacy and coloured oil droplets, yet it is not clear exactly how well birds can discriminate the reflecting object colours that they encounter in nature. With behavioural experiments, we determined colour discrimination thresholds of chickens in bright and dim light. We performed the experiments with two colour series, orange and green, covering two parts of chicken colour space. These experiments allowed us to compare behavioural results with model expectations and determine how different noise types limit colour discrimination. At intensities ranging from bright light to those corresponding to early dusk (250–10 cd m^{-2}), we describe thresholds accurately by assuming a constant signal-to-noise ratio, in agreement with an invariant Weber fraction of Weber's law. Below this intensity, signal-to-noise ratio decreases and Weber's law is violated because photon-shot noise limits colour discrimination. In very dim light (below 0.05 cd m^{-2} for the orange series or 0.2 cd m^{-2} for the green series) colour discrimination is possibly constrained by dark noise, and the lowest intensity at which chickens can discriminate colours is 0.025 and 0.08 cd m^{-2} for the orange and green series, respectively. Our results suggest that chickens use spatial pooling of cone outputs to mitigate photon-shot noise. Surprisingly, we found no difference between colour discrimination of chickens and humans tested with the same test in bright light.

KEY WORDS: Animal behaviour, Bird vision, *Gallus gallus*, Psychophysics, Visual modelling

INTRODUCTION

Birds use colour vision for many tasks, such as finding food and choosing between mating partners (Bennett and Cuthill, 1994; Cuthill et al., 1999). Bird colour vision is mediated by four single cone photoreceptors sensitive to red light (long-wavelength sensitive, LWS), green light (medium-wavelength sensitive, MWS), blue light (short-wavelength sensitive, SWS) and violet or ultraviolet light (very-short-wavelength sensitive, VS/UVS) (Osorio et al., 1999; Hart, 2001). Bird cones are equipped with coloured oil droplets that act as long-pass filters, which narrow spectral sensitivity and reduce the overlap in sensitivity between cone types. These retinal specializations are thought to improve colour discrimination (Barlow, 1982; Govardovskii, 1983; Vorobyev, 2003) and have inspired the hypothesis that bird colour discrimination abilities should be superior to those of most other vertebrates, including trichromatic humans (Vorobyev et al., 1998).

Discrimination of narrow-banded spectral lights has been studied in some bird species (e.g. Maier, 1992; Prescott and Wathes, 1999; Goldsmith and Butler, 2003; Goldsmith and Butler, 2005; Lind et al., 2014). These studies suggest that bird colour vision is tetrachromatic, mediated by the single cones, which are compared in opponent processing and well described as being limited by receptor noise (Vorobyev and Osorio, 1998). However, most natural colour stimuli are not narrow-banded spectral lights, but broad-banded object reflectances, and the discrimination thresholds for such object colours have never been tested in birds.

By absorbing light, the oil droplets not only narrow the spectral sensitivity, but also reduce absolute sensitivity of cones, which could affect colour discrimination in dim light (Vorobyev, 2003). The intensity threshold for colour vision has been tested in only three bird species, and they lose colour vision at higher intensities compared with humans (Lind and Kelber, 2009a; Gomez et al., 2014).

We assume that discrimination thresholds of visual systems are set by noise (Vorobyev and Osorio, 1998; Lind and Kelber, 2009b), and that noise can arise from different sources in different light conditions. Over a wide range of relatively high light intensities, we expect that Weber's law holds, so that sensitivity changes proportionally to light intensity and a constant Weber fraction (ω) describes the signal-to-noise ratio that sets discrimination thresholds (Donner et al., 1990; Osorio et al, 2004; Lind et al., 2014). Under these conditions, the main source of noise is probably transducer noise (Lillywhite and Laughlin, 1979; Howard and Snyder, 1983) originating at the later stages of signal transduction in the photoreceptors, possibly by fluctuations in cGMP levels (Angueyra and Rieke, 2013). There are no electrophysiological measurements of noise in bird photoreceptors, but rough estimates of noise have been deduced from the results of behavioural experiments on spectral sensitivity (Maier, 1992; Vorobyev et al., 1998; Lind et al., 2014).

At lower intensities, photon-shot noise and dark noise gain relative importance and lead to lower signal-to-noise ratios and thus a violation of Weber's law (Osorio et al., 2004). Photon-shot noise is caused by the stochastic nature of photon arrival that follows Poisson statistics. For a photon sample size N, the uncertainty is $\sqrt{N}$, and the signal-to-noise ratio is $N/\sqrt{N}$, which is the de Vries–Rose law (de Vries, 1943; Rose, 1942; Rose, 1948). It is proposed that visual systems can use spatial pooling to reduce the effect of photon-shot noise (e.g. Warrant, 1999). Pooling of signals from several photoreceptors increases signal strength (N) and signal-to-noise ratio, at the cost of spatial resolution. The absolute threshold of vision is set by dark noise (X), which originates from spontaneous activity in the photoreceptor that is indistinguishable from real photon absorption (Barlow, 1956; Rieke and Baylor, 1998; Rieke and Baylor, 2000). The signal-to-noise ratio of dark noise is expressed as $N/\sqrt{X}$.

We used the chicken (*Gallus gallus* Linnaeus 1758) to test how well birds can discriminate object colours in different light intensities. For comparison, we tested human subjects under the same conditions. We also compared the chickens' performance with predictions from an established colour vision model, the receptor-

[1]Lund University, Department of Biology, Sölvegatan 35, SE-226 32 Lund, Sweden. [2]Lund University, Department of Philosophy, SE-221 00 Lund, Sweden. [3]The University of Auckland, Department of Optometry and Vision Science, Auckland 1142, New Zealand.

*Author for correspondence (peter.olsson@biol.lu.se)

Received 16 July 2014; Accepted 4 November 2014

The Journal of Experimental Biology

The Journal of Experimental Biology (2014) doi:10.1242/jeb.111187

List of symbols and abbreviations

d	photoreceptor aperture diameter
D	pupil diameter
f	focal length of the eye
I	illumination spectrum
JND	just-noticeable difference
K	absorption coefficient
l	outer-segment length
L	non-normalized receptor spectral sensitivity
LWS	long-wavelength sensitive
MWS	medium-wavelength sensitive
N	absolute quantum catch
Q	relative quantum catch
R	normalised receptor spectral sensitivity
RNL	receptor-noise limited
S	reflectance spectrum
SWS	short-wavelength sensitive
VS	very-short-wavelength sensitive
X	dark noise rate
Δf	contrast in a receptor channel
Δt	integration time
κ	electrical conversion coefficient
λ	wavelength
σ	standard deviation of noise in a receptor
τ	ocular media transmission
ω	Weber fraction

noise-limited (RNL) model (Vorobyev and Osorio, 1998). This allowed us to address the following questions: (1) which Weber fraction – and thus receptor noise level – explains chicken colour discrimination thresholds in bright light best? (2) Over which intensity range is Weber's law valid for chicken colour discrimination? (3) What is the intensity limit of chicken colour vision? (4) Which types of noise are important for colour vision at different light intensities? (5) Can birds discriminate smaller colour differences than humans?

RESULTS

Colour discrimination in bright light

We trained newly hatched chicks to extract food crumbs from coloured food containers and tested how well they could discriminate a rewarded colour from unrewarded colours in two alternative choice tests. We trained eight chicks to discriminate between yellow and orange colours (orange series; Fig. 1A) and another group of eight chicks to discriminate between blue and green colours (green series; Fig. 1B). The unrewarded colours were chosen such that the colour difference to the rewarded colour ranged from well below 1 to above 3 just-noticeable differences (JNDs; see supplementary material Table S1), according to the RNL model, using a Weber fraction of 0.1 (Eqn 1 in the Materials and methods) for the LWS mechanism that is commonly adopted for birds (Vorobyev and Osorio, 1998; Lind et al., 2014). Colour differences larger than 1 JND should be discriminable if correct parameters are assumed and the model correctly describes behaviour (Vorobyev et al., 2001; Lind et al., 2014).

The chicks first learned to discriminate the largest colour differences (O5-O+ and G5-G+, Fig. 1) at 250 cd m^{-2}, and were then tested with progressively smaller colour differences. They easily discriminated all colour differences above 1 JND making between 80 and 100% correct choices. Discrimination performance dropped rapidly for smaller colour differences, and the thresholds were found to be 0.70±0.002 (mean ± s.d.) JNDs for the orange series and 0.58±0.03 JNDs for the green series (Fig. 1A,B).

We repeated the test at 10 cd m^{-2} and the colour discrimination thresholds 0.69±0.06 JND and 0.56±0.05 JND for the orange and green series, respectively, did not differ significantly from those at 250 cd m^{-2} (Fig. 1C,D). These results suggest that our initial assumptions of noise levels were too high. The Weber fraction that best explains the observed thresholds at both light intensities is 0.06, for the LWS mechanism. This is the Weber fraction we included in subsequent model calculations (Eqns 6 and 7).

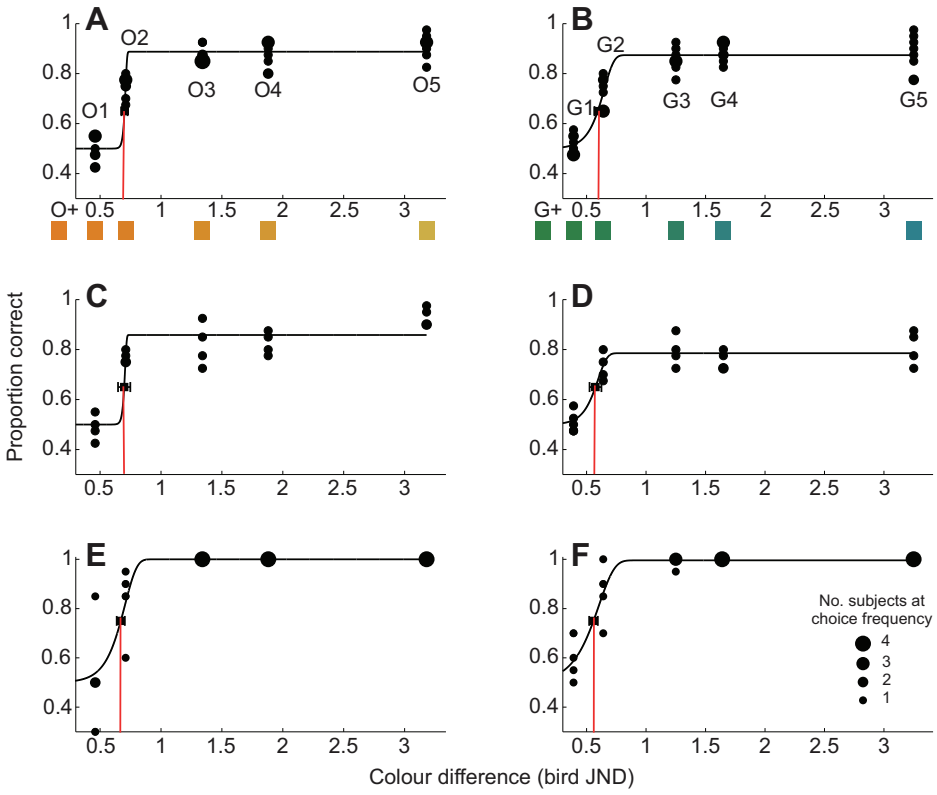

Fig. 1. Colour discrimination by chickens and humans in bright light. (A–D) The discrimination performance of chicks (n=8) for the orange (left column) and green (right column) series of colour stimuli. The x-axis gives colour difference in the unit of JND, as modelled assuming chicken colour vision and a Weber fraction of 0.1 for the LWS channel (Eqn 1). Chicks tested at (A,B) 250 cd m^{-2} and (C,D) 10 cd m^{-2}. (E,F) Human discrimination performance (n=4), plotted on the same scale for colour differences as for the chicks. Each filled circle refers to the fraction of correct choices made for the last 40 choices for chicks and 20 choices for humans at a given colour difference. The size of the circle corresponds to the number of subjects at a given choice level. The lines are psychometric functions fitted to the data of the group (see the Materials and methods). The boxes and red lines refer to the threshold. The inserts visualize the appearance of the colour stimuli. Versions of the data with fits to individual performance is available in supplementary material Fig. S1.

The Journal of Experimental Biology (2014) doi:10.1242/jeb.111187

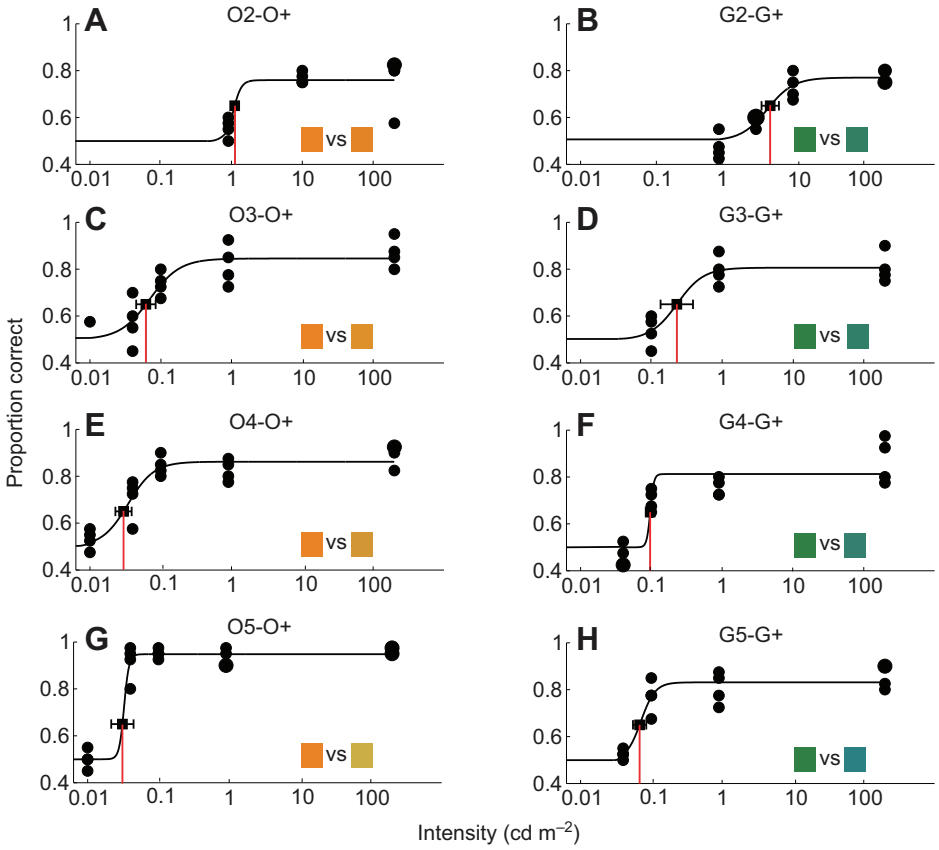

Fig. 2. Colour discrimination by chickens in dim light. The discrimination performance of chicks (*n*=4) for the four colour differences discriminable in bright light (see Fig. 1) in dimmer illumination for the orange series (left column) and the green series (right column). The boxes and red lines give threshold values at 65% correct choices, the circles refer to the level of performance of the chicks, and circle size corresponds the number of individuals at that level. The lines are psychometric functions fitted to the data of the group. Versions of the data with fits to individual performance are available in supplementary material Fig. S2.

For comparison, we asked two female and two male humans with normal colour vision to participate in the same colour discrimination experiments. Humans could discriminate the same colours as chicks; their thresholds, 0.66±0.03 and 0.54±0.04 chicken JNDs for the orange and green series, respectively, were similar to those of the birds (0.70±0.002 and 0.58±0.03) (Fig. 1E,F). Human thresholds fit well with modelled (RNL model) discriminability of the stimuli in human colour vision, using published data on Weber fractions for each cone mechanism (Wyszecki and Stiles, 2000).

Colour discrimination in dim light

We then tested chicken colour discrimination in even dimmer light, at 3, 0.9, 0.1, 0.04 and 0.01 cd m^{-2}, to find the intensity threshold for each colour pair that the chicks could discriminate in bright light (Fig. 2). Performance generally remained high until it dropped rapidly, close (within 1 log unit) to the intensity threshold. In both series, the intensity threshold was lower for larger colour differences between stimuli, but this effect declined dramatically for the largest colour differences (Fig. 2C–H and Fig. 3A,B). The intensity thresholds were consistently lower for the orange than for the green series. The intensity threshold for discrimination of the largest colour difference in the orange series was 0.025±0.008 cd m^{-2} and 0.080±0.027 cd m^{-2} for the green series.

Human subjects were asked to discriminate O5 from O+ and G5 from G+ at several intensities; their intensity threshold was lower than that of the chicks (see supplementary material Fig. S3). For human subjects, just as for birds, the intensity threshold was lower for the orange series than for the green series (see supplementary material Fig S3).

Intensity thresholds, Weber's law and absolute quantum catch

Using the RNL model we found that Weber's law and an invariant Weber fraction (0.06 for the LWS mechanism) did not explain the intensity thresholds for the discrimination of each colour pair at light intensities below 10 cd m^{-2}. We had to assume higher noise levels for the model to describe the behavioural thresholds (Fig. 3A–D). We assumed that photon-shot noise and dark noise caused the increase in noise level. The effects of photon-shot noise and dark noise depend on absolute quantum catches (N) of photoreceptors (Eqn 5), the calculation of which require anatomical and physiological data. Using the information given in Table 1 we determined the absolute quantum catches of individual photoreceptors looking at the colour stimuli at the tested intensities (Table 2; supplementary material Tables S2 and S3).

The effects of photon-shot noise and dark noise

Next, we modelled the effects of photon-shot noise and dark noise using the data on absolute quantum catches. First, we considered the addition of photon-shot noise (Eqn 6). Without spatial pooling, photon-shot noise levels are too high to explain the observed intensity thresholds (Fig. 3B,C). Spatial pooling improves signal-to-noise ratio and thus colour discrimination in dim light (Fig. 4A,B). We included spatial pooling in the model by multiplying absolute quantum catches in each receptor channel with the relative amount of spatial pooling (see Materials and methods for more information) (Fig. 3C,D and Fig. 4A,B).

In line with expectations (Barlow, 1958), we found that we needed to assume higher degrees of spatial pooling to explain the behavioural results for all but the most contrasting colour pairs at dimmer light intensities (Fig. 4A,B). In contrast, we found that to explain the

The Journal of Experimental Biology (2014) doi:10.1242/jeb.111187

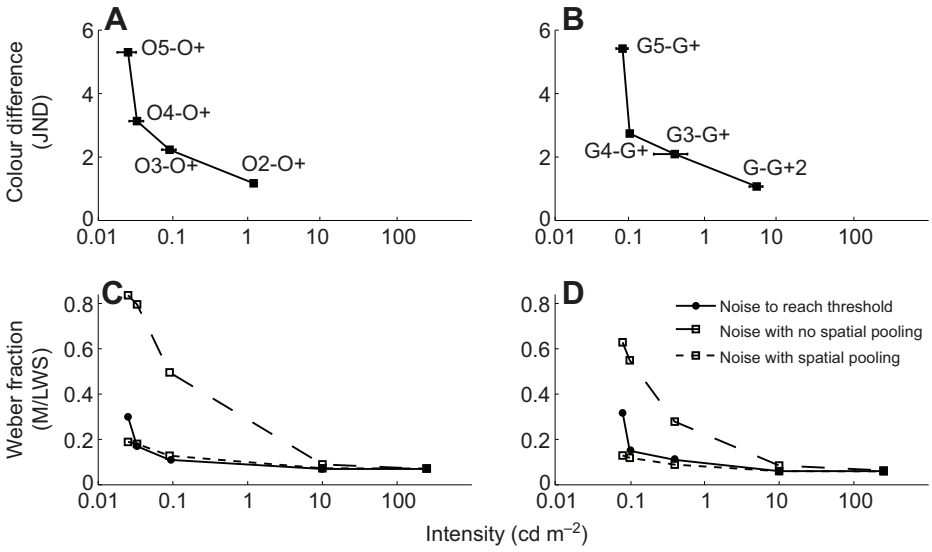

Fig. 3. Intensity thresholds and noise. (A,B) Mean (±s.d.) intensity thresholds for the colour differences in the orange and green series, respectively. Colour differences are modelled assuming a 0.06 Weber fraction for the LWS channel. (C,D) Weber fraction for the LWS channel required to consolidate the modelled colour difference of a given colour task with their respective intensity threshold (solid lines). The Weber fraction obtained assuming the addition of photon shot noise (Eqn 6) without spatial pooling (long dashed lines, assuming an integrative field containing 1 VS, 2 SWS, 4 MWS, 4 LWS cones), or with spatial pooling in a 25-fold integrative field (short dashed lines, 25 VS, 50 SWS, 100 MWS, 100 LWS) between the rewarded colour and each unrewarded colour in the orange and green series, respectively.

discrimination of the largest colours differences in each series (O5-O+ and G5-G+) we had to assume considerably less spatial pooling than for all other colour differences at higher light intensities. To explain this inconsistency, we also considered the effects of dark noise.

We adopted two approaches of taking the effects of dark noise into account. The first approach assumes linear signal transfer from the photoreceptors, meaning that there is equal pooling of false dark events and true photon catches, and resulting in one Weber fraction for each level of pooling (Eqn 7). Because dark noise levels are unknown for bird cone photoreceptors, we modelled dark noise levels between 10 and 600 events per second (Fig. 4C,D). The larger the rate of dark noise, the more spatial pooling was required to model the behavioural threshold (Fig. 4C,D). However, this approach again indicated that less spatial pooling should be required to explain the intensity thresholds of the largest colour differences (O5-O+ and G5-G+; supplementary material Fig. S6).

Therefore, in a second approach, we assumed nonlinear signal transfer from the photoreceptors (Field and Rieke, 2002). This way, dark noise sets a threshold quantum catch, in individual photoreceptors, that a light signal must surpass in order to be conveyed. To estimate this threshold, we plotted the absolute quantum catches of individual photoreceptors from the unrewarded colours at various intensity levels (see supplementary material Fig. S4). We estimated the dark noise threshold by the absolute quantum catches of individual photoreceptors from the stimuli at the dimmest light intensities. In the orange series, the MWS photoreceptor sees the largest difference in quantum catch between the rewarded and unrewarded stimuli; in the green series, it is the VS photoreceptor. Absolute quantum catch of a single MWS cone is ca. 7 and 9 per second from O+ and O4, respectively, at the intensity threshold of O4-O+, and 6 and 9 per second from O+ and O5 respectively, at the intensity threshold of O5-O+. Absolute quantum catch of a single VS cone is ca. 4 and 5 per second from G+ and G4, respectively, at the intensity threshold and 3 and 5 per second from G+ and G5, respectively, at the intensity threshold of G5-G+ (Fig. 4E,F; Table 2 and see supplementary material Tables S2 and S3). If we assume that a signal-to-noise ratio of 1 sets the threshold, and follow the calculations from Donner (Donner, 1989) (Eqn 8), our results suggest that a chicken MWS cone has a dark noise rate in the range of ~30–70 events per second and a VS cone has a dark noise rate of ~6–30 events per second.

Table 1. Values of parameters used for modelling absolute quantum catches

Parameter (unit)	Value	Ref.
Cone outer segment length (μm)	30	This study
Absorption coefficient	0.035	Bowmaker et al., 1977
Ellipsoid diameter (μm)	3.1	This study
Focal length (μm)	8300	This study
Pupil diameter (max–min) (μm)	4900–3500	This study
F-number (min)	1.66	This study
Transmission of ocular media τ (%)	80	Johnsen, 2012
Quantum transduction efficiency κ (%)	50	Johnsen, 2012
Integration time (max–min) (ms)	50–12	Lisney et al., 2011
Max. optical sensitivity S_w (μm^2 sr)	0.67	This study

DISCUSSION

Colour discrimination thresholds in bright light and the Weber fraction

Our results allow us, for the first time, to compare the predictions of the RNL model to behavioural discrimination thresholds for object

Table 2. Quantum catches of single receptor types per integration time

		Quantum catch (photons)			
Intensity (cd m^{-2})	Stimulus	LWS	MWS	SWS	VS
250	O+	1234	492	349	169
10	O+	180	72	51	25
0.9	O+	24	9.2	2.4	1.5
0.1	O+	2.7	1.1	0.6	0.2
0.04	O+	1.1	0.4	0.2	0.07
0.01	O+	0.3	0.1	0.07	0.02
250	G+	447	537	476	213
10	G+	65	78	70	31
0.9	G+	7.1	8.1	2.8	1.8
0.1	G+	0.8	0.9	0.7	0.2
0.04	G+	0.3	0.4	0.3	0.08
0.01	G+	0.09	0.1	0.08	0.02

Values are calculated from the rewarded colour stimulus in the orange and green series in the different intensity levels using Eqn 5 and values from Table 1. Excerpt of full tables available in supplementary material Tables S2 and S3. D=0.350, 0.415, 0.466, 0.472, 0.477 and 0.499 cm; Δt=0.012, 0.025, 0.05, 0.05, 0.05 and 0.05 s for the intensities, 250, 10, 0.9, 0.1, 0.04 and 0.01 cd m^{-2}, respectively.

The Journal of Experimental Biology (2014) doi:10.1242/jeb.111187

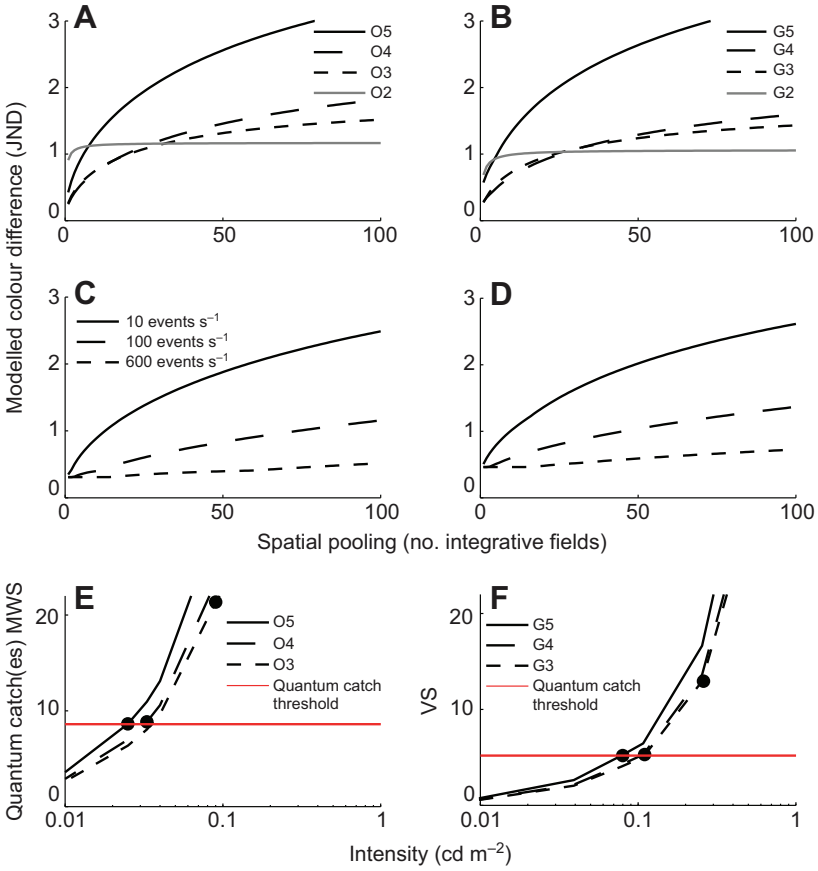

Fig. 4. The effect of photon-shot noise and dark noise on intensity thresholds of chicken colour vision. (A–D) The modelled colour difference between rewarded and unrewarded colours at their intensity thresholds assuming different levels of spatial pooling. The model predictions agree with the behavioural data when the modelled colour difference reaches 1 JND. An integrative field contains 1 VS, 2 SWS, 4 MWS and 4 LWS cones, a twofold integrative field contains 2 VS, 4 SWS, 8 MWS and 8 LWS cones, etc. (A,B) Weber fractions are set by photon-shot noise (Eqn 6) combined with spatial pooling. (A) The colours in the orange series O5, O4, O3 and O2 modelled at 0.025, 0.033, 0.09 and 10 cd m^{-2}, respectively. The degree of spatial pooling required to reach threshold (1 JND) is 2, 20, 20 and 6-fold integrative fields for O2, O3, O4 and O5. (B) The colours in the green series, G5, G4, G3 and G2 modelled at 0.08, 0.1, 0.26 and 10 cd m^{-2}. The degree of spatial pooling required to reach threshold (1 JND) is 11, 24, 26 and sixfold integrative fields for G2, G3, G4 and G5. (C,D) Weber fractions are set by photon-shot noise and dark noise (Eqn 7) combined with spatial pooling. (C) O5 at 0.025 cd m^{-2}, at four different levels of dark noise. (D) G5 modelled at 0.08 cd m^{-2}, at four different levels of dark noise. (E) The absolute quantum catches (per second) of a single MWS cone from O5, O4 and O3 at various intensities. (F) The absolute quantum catches of a single VS cone from G5, G4 and G3 at various intensities. The red lines in E and F show proposed quantum catch thresholds.

colours in bright and dim light in birds. Initially, we assumed a noise level corresponding to a Weber fraction of 0.1 for the LWS channel, as suggested from behavioural tests of spectral sensitivity in the pekin robin (*Leiothrix lutea*) (Maier and Bowmaker, 1993; Vorobyev and Osorio, 1998) and the budgerigar (*Melopsittacus undulatus*) (Lind et al., 2014). To describe the chicks' performance in bright light, in 250 and 10 cd m^{-2}, and to set the observed discrimination threshold to 1 JND, we have to assume a lower Weber fraction of 0.06.

If chickens truly have lower receptor noise levels than budgerigars, this could also help to explain their higher contrast sensitivity (7% Michelson contrast) (Schmid and Wildsoet, 1998; Jarvis et al., 2009), compared with budgerigars (11% Michelson contrast) (Lind and Kelber, 2011). Another explanation could be that exploiting the natural chicken behaviour – pecking at objects on the ground to get food – may facilitate better performance than using the artificial task of associating food with spectral lights as with the pekin robins and budgerigars (Maier and Bowmaker, 1993; Lind et al., 2014).

Intensity range of Weber's law

In a recent study on budgerigars, behavioural spectral sensitivity data could be explained with a constant Weber fraction over a wide range of background intensities above 1 cd m^{-2}, whereas other noise sources had to be taken into account at lower intensities (Lind et al., 2014). Our current study of object colour discrimination in chickens shows that an invariant Weber fraction describes thresholds at both 250 and 10 cd m^{-2}, whereas noise increases at lower intensities (Fig. 3C,D). Similar to these results, colour discrimination thresholds in humans increase strongly at intensities below ~3 cd m^{-2} compared with brighter light intensities (Brown, 1951; Yebra et al., 2000).

The absolute intensity limit of colour discrimination

We used the intensity thresholds for the orange and green stimulus pairs O5-O+ and G5-G+ (colour differences are 5.3 and 5.4 JNDs, respectively, with a Weber fraction of 0.06 for the LWS mechanism; Fig. 2G,H; Fig. 3A,B) as estimates of the absolute intensity limit of colour discrimination. We found that the intensity threshold in the green series, 0.08 cd m^{-2}, of chickens was comparable to thresholds for blue–green colour discrimination of budgerigars (*Melopsittacus undulatus*), Bourke's parrots (*Neosephotus bourkii*) and blue tits (*Cyanistes caeruleus*), which could discriminate colours at 0.1 cd m^{-2}, 0.4 cd m^{-2} and between 0.05 and 0.2 cd m^{-2}, respectively (Lind and Kelber, 2009; Gomez et al., 2014). Our results show that the intensity threshold for colour discrimination depends on colour difference between the stimuli, but this dependence is reduced for colour differences larger than about 3 JND (Fig. 3A,B). In the blue tit study, the colour differences are very large, in the budgerigar and Bourke's parrot study colour differences are slightly smaller but above 4 JND (O.L., unpublished data) and thus also reflect absolute intensity thresholds. The intensity threshold for the orange series was lower, 0.025 cd m^{-2}, this is probably partly an effect of the orange series being generally brighter than the green series [*ca.* 1.5-times brighter for chicken double cones (O+/G+)]. Blue and green colours have band-pass characteristics and are therefore generally dimmer than orange and yellow colours (see supplementary material Fig. S5).

Colour discrimination in dim light: which sources of noise limit colour vision in dim light?

Photon-shot noise

Without spatial pooling, photon-shot noise was too large to explain the intensity thresholds we observed (Fig. 3C,D; Fig. 4A,B), even

at the intensity of 10 cd m^{-2}, where the colour discrimination threshold was similar to that in bright light (250 cd m^{-2}). In our model we needed to assume less spatial pooling (between two- and 11-fold integrative fields) to explain discrimination of the colour pairs O2-O+ and G2-G+, at 10 cd m^{-2} and more spatial pooling (20- to 25-fold integrative fields) to explain discrimination of O3-O+, G3-G+, O4-O+ and G4-G+ at dimmer light intensities. This fits the expectation that spatial pooling increases in lower light intensities (Barlow, 1958). However, the discrimination of the colour pairs O5-O+ and G5-G+ (with the largest differences from the respective rewarded colour) could be explained assuming considerably less spatial pooling (about six-fold integrative fields), which was puzzling and inconsistent with our expectations. We conclude that most likely, this inconsistency indicates that our model of dim light colour discrimination is too simplified, because it does not account for yet another source of noise, dark noise (Barlow, 1956).

Dark noise

Dark noise sets the ultimate intensity limit of vision (Barlow, 1956; Donner, 1992) but how it affects colour vision is unclear. The level of dark noise, defined by the rate of spontaneous photon-absorption-like events (dark events) in a single receptor, has been well described in rods and is usually in the range of 0.01 dark events per second (Rieke and Baylor, 1998). In cones, however, good estimates of dark noise are difficult to obtain, and range from fewer than 10 up to several thousands of events per second (Lamb and Simon, 1977; Schnapf et al., 1990; Donner, 1992; Schneeweis and Schnapf, 1995; Rieke and Baylor, 2000; Fu et al., 2008; Angueyra and Rieke, 2013). We could find no satisfactory fit to our behavioural data assuming linear signal transfer from the photoreceptors, despite modelling a large range of dark noise rates (see supplementary material Fig. S6).

Nonlinear signal transfer has been found in the rod–rod bipolar cell synapse (Field and Rieke, 2002), which provides a threshold in the synapse between the photoreceptor and the bipolar cell. This threshold rejects weak signals from the photoreceptor, thereby effectively removing false signal from dark events but also some real signal from captured photons. This apparent loss is counteracted by the benefit that only signal from real photon catch is transmitted to the bipolar cell. It is unknown whether this nonlinearity is also present in the cone pathway, or whether it is present at all in birds. However, the existence of such thresholds could help to explain our data. The sharp cut-off in the decrease of intensity threshold despite increasing colour difference (Fig. 3A,B) conforms to the idea that a threshold exists at the photoreceptor level. The intensity threshold of the two largest colour differences in each series may be set when they reach such a threshold in quantum catch and we estimate this threshold to be ~5–10 photons per second (red lines in Fig. 4E,F). Although our estimates of dark noise rate are coarse, they are in line with the idea that the λ_{max} of the photoreceptor is important for its dark noise rate (Barlow, 1957; Firsov and Govardovskii, 1989; Rieke and Baylor, 2000; Ala-Laurila et al., 2004).

Can birds discriminate smaller colour differences than humans?

Chickens and humans performed equally well in our colour discrimination experiments. It seems that colour discrimination performance within the human visual range (about 400–700 nm) is similar in humans and birds, an idea also suggested by Lind et al. (Lind et al., 2014). The Weber fraction for human LWS cone photoreceptors has been suggested to be 0.018 (Wyszecki and Stiles, 2000), which is much smaller than the Weber fraction for bird LWS cones (0.06 for chickens and 0.1 for Leiothrix and budgerigars). This difference could explain why we found no obvious difference in colour discrimination threshold between humans and birds and may also help to explain why birds generally have lower contrast sensitivity than humans (Ghim and Hodos, 2006; Gover et al., 2009; Harmening et al., 2009; Lind et al., 2012).

Concluding remarks

The RNL model describes thresholds of colour discrimination accurately over a wide range of intensities, using realistic physiological assumptions. (1) For the chicken, Weber's law holds at least for intensities down to 10 cd m^{-2} with a Weber fraction of 0.06 for the LWS channel. (2) At lower light intensities photon-shot noise affects colour discrimination. To counteract the effect of photon-shot noise, the retina of birds must use spatial and temporal pooling. At very low light intensities, dark noise explains the intensity threshold of colour discrimination, by determining the minimum quantum catch for making single photoreceptors useful for vision. (3) The intensity threshold of colour discrimination depends on the amplitude of stimulus reflectance (brightness) and the difference in spectral composition between the stimuli; bright stimuli with large colour difference can be discriminated in lower light intensities. (4) Assuming that intensity thresholds of colour discrimination are set by photon-shot noise alone can overestimate the intensity threshold of large colour differences. (5) Birds and humans did not differ significantly in how they discriminated small colour differences, however humans could discriminate colours at lower light intensities than birds. Birds should still be able to see colours that humans cannot discriminate because their visual range extends into the ultraviolet region of the spectrum. Taken together, our results add understanding of the process underlying colour discrimination thresholds, and allow for more realistic and reliable modelling of colour discrimination in natural contexts, both in bright and dim light.

MATERIALS AND METHODS

Animals

Chicks of the Lohman White breed were obtained as eggs from a local breeder (Gimranäs AB, Herrljunga, Sweden), hatched in a commercial incubator (Covatutto 24, Högberga AB, Matfors, Sweden) and housed in 12 h:12 h light:dark cycle. Animals were kept in accordance with regulations specified by the Swedish board of Agriculture and approved for housing by the same agency (Reg. no. 6.2.18-8245/13). Experiments were approved by the responsible ethical committee (Reg. no. 6-12). Both male and female chicks were used in the experiments. During training and testing, the birds were fed only during the experiment; at the end of the day, they were allowed a full feeder that was removed on the following morning at least 2 h before experiment. The birds were about 3 weeks old when they finished the bright light experiment and about 5 weeks old when they finished the dim light experiment.

Illumination

The experimental cage (70×40 cm wooden box) was illuminated from above by fluorescent tubes (Biolux L18W/965; Osram, München, Germany) at 250 cd m^{-2} and 10 cd m^{-2} and white LEDs (white 5 mm, 20 cd; Kjell & Company, Malmö, Sweden) at all lower light intensities (Fig. 5). The intensity of the illumination was measured from a white paper on the floor of the cage using a radiometer (ILT1700 Research Radiometer, International Light, Peabody, MA, USA). The illumination radiance spectrum was measured from a white standard on the floor of the experimental cage with a calibrated spectroradiometer (RSP900-R; International Light, Peabody, MA, USA). The radiance spectrum at intensities below 3 cd m^{-2} was determined by scaling the radiance measurements according to the radiometric measurements. We used seven

The Journal of Experimental Biology (2014) doi:10.1242/jeb.111187

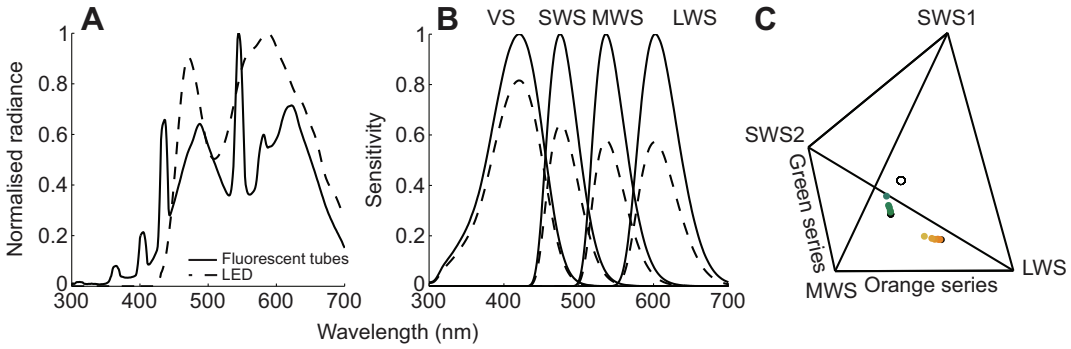

Fig. 5. Illumination spectra, chicken cone sensitivity and chromaticity diagram. (A) The radiance spectrum of the fluorescent tubes (solid line) and the LEDs (dashed line) at 250 and 3 cd m^{-2} respectively. The maxima of the normalised spectra refer to 1.5×10^{11} photons cm^2 s^{-1} sr^{-1} (fluorescent tubes) and 1.5×10^{9} photons cm^2 s^{-1} sr^{-1} (LEDs). (B) The spectral sensitivity of the four single cones in the chicken retina, accounting for oil droplet and ocular media filtering. The solid lines represent the normalized sensitivity used to determine relative quantum catch in bright light, the dashed lines represent the lower sensitivity resulting from oil droplet and ocular media filtering, used to calculate absolute quantum catch in dim light. (C) The loci of the two colour series in a chicken chromaticity diagram, assuming no adaptive background. The black circles refer to the rewarded colour in each series, the orange on the right side and the green on the left. The open circle represents the achromatic point.

intensity levels: 250 cd m^{-2}, 10 cd m^{-2}, 3 cd m^{-2}, 0.9 cd m^{-2}, 0.11 cd m^{-2}, 0.04 cd m^{-2} and 0.01 cd m^{-2}.

Stimuli

The stimuli were adapted from a previous study (Osorio et al., 1999). Colours were created in Adobe Illustrator, Creative Suite package version 5, using CMYK colour coding. We created rectangles measuring 30×35 mm that were subdivided into 90 small rectangles measuring 2×6 mm. A random subset (30%) of the small rectangles were coloured and the remaining 70% had shades of grey of random (0.3 Michelson contrast range for the double cone) intensity. These patterns were printed on paper and folded into conical food containers. Two series of colours were created to test two parts of chicken colour space and variation for different receptor types (Table 1; Fig. 5C). In order to find behavioural thresholds, the colours in each series were chosen to lie in a line in the tetrachromatic colour space, thus generating a range of colour differences between the rewarded and the unrewarded colours. The black ink value of the colour rectangles was varied randomly to yield intensity variation over a 0.05−0.17 Michelson contrast range to make intensity an unreliable cue. The maximum contrast between an average intensity colour stimulus and the average intensity of the grey fields was 0.09 Michelson contrast for the double cone. The brightness contrast between the colours (the brightest version of each stimulus) within each series was lower than 10% (Michelson contrast) for the chicken double cones, thus below their brightness discrimination threshold (Jones and Osorio, 2004), in all conditions.

In bright light the radiance spectrum (R and I in Eqn 2 are already combined in the measurement) of the colours was measured directly from a paper with printed colour. However, for the dim light experiment the spectroradiometer was not sensitive enough to measure the colours directly. Therefore the reflectance (see supplementary material Fig. S5) of the colours was measured under a broad-spectrum Xenon light source (HPX-2000-HP-DUV, Ocean Optics, Dunedin, FL, USA), with a spectrometer (Maya 2000, Ocean Optics, Dunedin, FL, USA) and combined with the radiance spectrum of the illumination to reconstruct the radiance spectra of the colours in dim light.

Visual modelling of performance in bright light

Colour differences were calculated using the RNL model proposed by Vorobyev and Osorio (Vorobyev and Osorio, 1998). Photoreceptor sensitivities (Fig. 5B) were modelled by combining known peak absorbance of the chicken cone visual pigments with the transmittance data for oil droplets and ocular media (Bowmaker et al., 1997; Lind and Kelber, 2009a) using the template by Govardovskii et al. (Govardovskii et al., 2000). Human visual pigments were modelled with the Govardovskii template, using the absorbance peaks of human visual pigments (Dartnall et al., 1983) including the filtering by human ocular media and macular pigment (Wyzecki and Styles, 2000) for the LWS and MWS cone (see supplementary material Fig. S7).

The RNL model assumes that the discrimination thresholds are set by photoreceptor noise, which is propagated into higher order processing. We assumed that spatial pooling can be used to improve signal-to-noise ratio so that a limiting Weber fraction for a receptor channel i can be calculated as:

$$\omega_i = \frac{\sigma_i}{\sqrt{\eta_i}}, \quad (1)$$

where ω is the Weber fraction, σ is the standard deviation of the noise in a single cone channel and η is the relative abundance of cone type i. The relative abundance of each cone type in chicken is 1:2:4:4 for the VS, SWS, MWS and LWS type, respectively (Kram et al., 2010). We initially assumed a standard deviation of noise of 0.2, which leads to a Weber fraction of 0.1 for the LWS and MWS channels as suggested for other birds, by Vorobyev and Osorio (Vorobyev and Osorio, 1998) and Lind et al. (Lind et al., 2014). However, for modelling discrimination in dim light we used the Weber fraction that resulted from our behavioural tests (Fig. 1).

The quantum catch Q of cone type i is given by:

$$Q_i = \int_{300}^{700} R_i(\lambda) S(\lambda) I(\lambda) \Delta\lambda, \quad (2)$$

where R is the spectral sensitivity of photoreceptor i (i = VS, SWS, MWS, LWS), S is the reflectance spectrum of the stimulus and I is the radiance spectrum of the illumination.

To model the discriminability of two stimuli, we then calculated the difference (Δf_i) in quantum catch between the stimuli for each cone type as:

$$\Delta f_i = \ln\left(\frac{Q_i \text{ stimulus 1}}{Q_i \text{ stimulus 2}}\right). \quad (3)$$

We assumed that the photoreceptors are appropriately adapted to the background for optimal performance.

The discriminability of two colour stimuli for a tetrachromatic animal, such as the chicken, was calculated as:

$$\Delta S^2 = \frac{\begin{aligned}&(\omega_1\omega_2)^2(\Delta f_4-\Delta f_3)^2+(\omega_1\omega_3)^2(\Delta f_4-\Delta f_2)^2\\&+(\omega_1\omega_4)^2(\Delta f_3-\Delta f_2)^2+(\omega_2\omega_3)^2(\Delta f_4-\Delta f_1)^2\\&+(\omega_2\omega_4)^2(\Delta f_3-\Delta f_1)^2+(\omega_3\omega_4)^2(\Delta f_2-\Delta f_1)^2\end{aligned}}{(\omega_1\omega_2\omega_3)^2+(\omega_1\omega_2\omega_4)^2+(\omega_1\omega_3\omega_4)^2+(\omega_2\omega_3\omega_4)^2}, \quad (4)$$

where ΔS is the colour difference (sometimes distance/chromatic contrast) in the unit of just noticeable differences (JND), where differences ≥1 JND are assumed to be discriminable (Vorobyev et al., 2001; Lind et al., 2014) .

Modelling colour differences in dim light, absolute quantum catch

To estimate photon-shot noise and dark noise we determined absolute quantum catch, N, for each receptor type, using the following equation:

$$N_i = \left(\frac{\pi}{4}\right)^2 \left(\frac{d}{f}\right)^2 D^2 \kappa \tau \Delta t \int_{300}^{700} \left(1 - e^{-kA(\lambda)l}\right) L(\lambda) \Delta\lambda \,, \quad (5)$$

where d is the diameter of the ellipsoid in the inner segment, f is the focal length of the eye, D is the pupil diameter, κ is the electrical conversion coefficient, which is set to 50%, τ is the absolute transmission of the ocular media independent of wavelength, which is set to 80%, Δt is the integration time of the photoreceptor (determined from the flicker fusion frequency measured by Lisney, 2011), A is cone sensitivity considering the reduction in quantum catch from the filtering of oil droplets and ocular media (dashed curve in Fig 5), k is the absorption coefficient, l is the length of the outer segment in μm, and L is the radiance of the stimulus (Johnsen, 2009). The values of f, D, d and l were determined as described below. The values we used are given in Table 2. The intensity-dependent radiance measurements L can be obtained from P.O. on request.

Photon-shot noise

We included photon-shot noise into the RNL model by using Equations 2, 3, and 4 but substituting the Weber fraction with the noise term from this equation:

$$\omega_{i,\text{photon}} = \frac{\sqrt{\omega_i^2 N_i^2 + N_i}}{N_i} \,, \quad (6)$$

where N is the average of the absolute quantum catches of the two stimuli compared and ω is the Weber fraction calculated from Eqn 1 of a receptor type i, estimated from our behavioural results (Fig. 1). We assumed that the retina of the bird can use spatial pooling to increase the absolute quantum catch N, and thereby the signal-to-noise ratio incurred by photon-shot noise. We assumed that the level of spatial pooling that can occur within a channel is determined by its relative abundance in the retina, similar to Vorobyev and Osorio (Vorobyev and Osorio, 1998). One set of single cones contains 1:2:4:4 VS, SWS, MWS and LWS cones, respectively, which represents relative cone abundance and without spatial pooling, this correlates to one integrative field. A twofold integrative field contains 2:4:8:8 VS, SWS, MWS and LWS cones, respectively, and so forth. The absolute quantum catch N of a given cone channel is then multiplied by the corresponding number of receptors of that type within the total integrative field.

Dark noise

We included the effect of dark noise to the RNL model by calculating a new Weber fraction as:

$$\omega_{i,\text{dark}} = \frac{\sqrt{\omega_i^2 N_i^2 + N_i + X_i}}{N_i} \,, \quad (7)$$

where X is the number of photon-equivalent dark events in the receptor channel i, and N is the absolute quantum catch and ω is the Weber fraction from Eqn 1 of receptor channel i, estimated from our behavioural results (Fig. 1). The effective X for a given channel was determined by multiplying the dark noise rate with the integration time of the photoreceptors and the number of cones of that type in the integrative field. To model colour difference including the effect of dark noise we used Eqns 2, 3 and 4 but substituted the Weber fraction by the noise term from Eqn 7. We assumed the same rate of dark noise for all receptor types and evaluated several rates of dark noise, 10, 100 and 600 dark events per second per cone.

To calculate the dark noise rate in a single receptor we used the equation from Donner (Donner, 1989):

$$\text{SNR} = \frac{N}{\sqrt{N + X}} \,, \quad (8)$$

where SNR is the signal-noise ratio, N is the quantum catch and X is the dark noise. We assumed that an SNR of 1 sets the threshold and then calculated the dark noise rate.

Anatomical data and pupil dynamics

The pupil diameters of three chickens were measured at ca. 5 weeks of age, at the intensities used in the study (see supplementary material Fig. S8). We attached a white spherical plastic marble to the head of the animals as a reference and filmed them with a video camera (Sony HDR-XR 500VE) in night-shot mode. At each intensity level, the largest pupil diameter D measured from each individual bird was used. The focal length f was determined from frozen sections of chicken eyes (ca. 5 weeks old) after the behavioural experiment, as previously reported in Lind and Kelber (Lind and Kelber, 2009b). The photoreceptor ellipsoid diameter d and outer segment length l were measured in transmission electron micrographs of some animals used in the behavioural studies at ca. 5 weeks of age.

Behavioural assays

Initial training of stimulus association

Forty-eight hours after hatching, the chicks were trained, in groups of 4 to 5 individuals, to associate food containers of the rewarded colour with food. The folded container contained a small portion of commercial chick crumbs that spilled out when the chick pecked at the container. On the second day the chicks were trained in pairs with the same tasks. The third day they were trained, in pairs, to walk out into the arena after a partition wall was removed to get access to a single food container. On the fourth day the same procedure was repeated but chicks were trained one by one.

Colour discrimination in bright light

From the fifth day onwards each chick was presented with a rewarded food container and an unrewarded food container of a different colour, for the first time. After the partition wall was removed, the chick was allowed to make one peck at one container. If the chick pecked at the container of the rewarded colour the food spilled out and the container with the unrewarded colour was removed. If it pecked the container of the unrewarded colour both containers were removed. The unrewarded colour that the chicks encountered first was the colour most different (O5-O+, or G5/G+, for the green series) from the rewarded colour. The two stimuli were separated by 5 cm. Each chick (n=8 for each series) had two training sessions with 20 trials per day, one in the morning and one in the afternoon. After a chick had reached 75% correct choices for two consecutive sessions indicating that it had learned the task, we continued with the unrewarding colour of the next smaller colour difference in the respective series. For all but one chick it took four sessions to reach our criterion; one chicken took five sessions to reach learning criterion. For each colour difference the animals had four sessions, data from the last two sessions were analysed.

Colour discrimination in dim light

The dim-light experiment started after the bright-light experiment was finished. In each series, the chicks were divided in two groups, four of them continued first with O5 (G5, for the green series) and then O3 (G3) as unrewarding colours in increasingly dim light intensities, the other four with O4 (G4) and then O2 (G2). They were first trained again in bright light, to a given colour difference for two sessions, the next day in the next lower intensity, and each following day the intensity was lowered further. Each animal had two sessions consisting of 20 presentations, at every intensity level. Prior to the experiment the birds were adapted to the intensity. We allowed different adaptation times according to the intensity level, 5, 7, 10, 15 and 15 min to 10, 0.9, 0.1, 0.4 and 0.01 cd m^{-2}, respectively.

Tests with human subjects

Four subjects (25–35 years old) with stated normal colour vision agreed to participate in a comparative experiment with the exact same stimuli and illumination conditions as with the chickens. Subjects were allowed 2 min to familiarize with the rewarded stimulus and then tested in a two-choice experiment starting in bright light and the largest colour difference (O/G5-O/G+). No positive feedback was given. Humans were allowed the same adaptation times as the birds for each intensity level.

Data analysis

For each animal, the percentage of correct choices of the last 40 choices for each task was plotted against the calculated colour difference or intensity.

We fitted a logistic function to the data using the Palamedes toolbox in Matlab (Prins and Kingdom, 2009). The fitted lines in Figs 1 and 2 are logistic functions fitted to the group data, and the thresholds reported in the text are means ± s.d. of thresholds derived via bootstrapping of the fitted function. We used a binomial test to decide on a threshold for discrimination at 65% correct choices (N=40, P<0.05, one-tailed binomial test) for chickens and a threshold of 75% for humans (N=20, P<0.05, one-tailed binomial test). We then altered the noise variable in the RNL model to consolidate the modelled threshold and the behavioural threshold, such that 1 JND coincides with the behavioural threshold.

Acknowledgements
We thank Christine Scholtyßek and two anonymous reviewers for helpful comments on earlier versions of the manuscript. We also thank our colleagues in the Vision Group at Lund University and our collaborators Joseph Corbo and Matthew Toomey from Washington University in St Louis and Nicholas Roberts and David Wilby from Bristol University for fruitful discussions.

Competing interests
The authors declare no competing financial interests.

Author contributions
A.K., O.L. and P.O. conceptualised the study. P.O. performed the experiments. A.K., O.L. and P.O. analysed and interpreted the data. P.O. wrote the manuscript with contributions from A.K. and O.L.

Funding
The work was funded by the Human Frontier Science Programme [RGP0017/2011], the Swedish Research Council [621-2009-5683, 2012-2212 and 637-2013-388] and the K A Wallenberg Foundation.

Supplementary material
Supplementary material available online at
http://jeb.biologists.org/lookup/suppl/doi:10.1242/jeb.111187/-/DC1

References

Ala-Laurila, P., Donner, K. and Koskelainen, A. (2004). Thermal activation and photoactivation of visual pigments. *Biophys. J.* **86**, 3653-3662.
Angueyra, J. M. and Rieke, F. (2013). Origin and effect of phototransduction noise in primate cone photoreceptors. *Nat. Neurosci.* **16**, 1692-1700.
Barlow, H. B. (1956). Retinal noise and absolute threshold. *J. Opt. Soc. Am.* **46**, 634-639.
Barlow, H. B. (1957). Purkinje shift and retinal noise. *Nature* **179**, 255-256.
Barlow, H. B. (1958). Temporal and spatial summation in human vision at different background intensities. *J. Physiol.* **141**, 337-350.
Barlow, H. B. (1982). What causes trichromacy? A theoretical analysis using comb-filtered spectra. *Vision Res.* **22**, 635-643.
Bowmaker, J. K. and Knowles, A. (1977). The visual pigments and oil droplets of the chicken retina. *Vision Res.* **17**, 755-764.
Bennett, A. T. and Cuthill, I. C. (1994). Ultraviolet vision in birds: what is its function? *Vision Res.* **34**, 1471-1478.
Brown, W. R. J. (1951). The influence of luminance level on visual sensitivity to color differences. *J. Opt. Soc. Am.* **41**, 684-688.
Cuthill, I. C., Bennet, T. D., Partridge, J. C. and Maier, E. J. (1999). Plumage reflectance and the objective assessment of avian sexual dichromatism. *Am. Nat.* **153**, 183-200.
Dartnall, H. J. A., Bowmaker, J. K. and Mollon, J. D. (1983). Human visual pigments: microspectrophotometric results from the eyes of seven persons. *Proc.R. Soc. B* **220**, 115-130.
De Vries, H. L. (1943). The quantum character of light and its bearing upon threshold of vision, the differential sensitivity and visual acuity of the eye. *Physica* **10**, 553-564.
Donner, K. (1989). The absolute sensitivity of vision: can a frog become a perfect detector of light-induced and dark rod events? *Physica Scripta* **39**, 133-140.
Donner, K. (1992). Noise and the absolute thresholds of cone and rod vision. *Vision Res.* **32**, 853-866.
Donner, K., Copenhagen, D. R. and Reuter, T. (1990). Weber and noise adaptation in the retina of the toad *Bufo marinus*. *J. Gen. Physiol.* **95**, 733-753.
Field, G. D. and Rieke, F. (2002). Nonlinear signal transfer from mouse rods to bipolar cells and implications for visual sensitivity. *Neuron* **34**, 773-785.
Firsov, M. and Govardovskii, V. (1989). Dark noise of visual pigments with differing location of absorption maxima. *Sensornye Sistemy* **4**, 25-34.
Fu, Y., Kefalov, V., Luo, D. G., Xue, T. and Yau, K. W. (2008). Quantal noise from human red cone pigment. *Nat. Neurosci.* **11**, 565-571.
Ghim, M. M. and Hodos, W. (2006). Spatial contrast sensitivity of birds. *J. Comp. Physiol. A* **192**, 523-534.
Goldsmith, T. H. and Butler, B. K. (2003). The roles of receptor noise and cone oil droplets in the photopic spectral sensitivity of the budgerigar, *Melopsittacus undulatus*. *J. Comp. Physiol. A* **189**, 135-142.
Goldsmith, T. H. and Butler, B. K. (2005). Color vision of the budgerigar (*Melopsittacus undulatus*): hue matches, tetrachromacy, and intensity discrimination. *J. Comp. Physiol. A* **191**, 933-951.
Gomez, D., Arnaud, G., Del Rey Granado, M., Bassoul, M. and Degueldre, D. Perret, P. and Doutrelant, C. (2014). The intensity threshold of colour vision in a bird, the blue tit. *J. Exp. Biol.* **217**, 3775-3778.
Govardovskiĭ, V. I. (1983). On the role of oil drops in colour vision. *Vision Res.* **23**, 1739-1740.
Govardovskii, V. I., Fyhrquist, N., Reuter, T., Kuzmin, D. G. and Donner, K. (2000). In search of the visual pigment template. *Vis. Neurosci.* **17**, 509-528.
Gover, N., Jarvis, J. R., Abeyesinghe, S. M. and Wathes, C. M. (2009). Stimulus luminance and the spatial acuity of domestic fowl (*Gallus g. domesticus*). *Vision Res.* **49**, 2747-2753.
Harmening, W. M., Nikolay, P., Orlowski, J. and Wagner, H. (2009). Spatial contrast sensitivity and grating acuity of barn owls. *J. Vision* **9**, 1-12.
Hart, N. S. (2001). The visual ecology of avian photoreceptors. *Prog. Retin. Eye Res.* **20**, 675-703.
Howard, J. and Snyder, A. W. (1983). Transduction as a limitation on compound eye function and design. *Proc. R. Soc. B* **217**, 287-307.
Jarvis, J. R., Abeyesinghe, S. M., McMahon, C. E. and Wathes, C. M. (2009). Measuring and modelling the spatial contrast sensitivity of the chicken (*Gallus g. domesticus*). *Vision Res.* **49**, 1448-1454.
Jones, C. D. and Osorio, D. (2004). Discrimination of oriented visual textures by poultry chicks. *Vision Res.* **44**, 83-89.
Johnsen, S. (2012). Absorption. In *The Optics of Life* (ed. S. Johnsen), pp. 104-115. Princeton, NJ: Princeton University Press.
Kelber, A. and Lind, O. (2010). Limits of colour vision in dim light. *Ophthalmic Physiol. Opt.* **30**, 454-459.
Kram, Y. A., Mantey, S. and Corbo, J. C. (2010). Avian cone photoreceptors tile the retina as five independent, self-organizing mosaics. *PLoS ONE* **5**, e8992.
Lamb, T. D. and Simon, E. J. (1977). Analysis of electrical noise in turtle cones. *J. Physiol.* **272**, 435-468.
Lillywhite, P. G. and Laughlin, S. B. (1979). Transducer noise in a photoreceptor. *Nature* **277**, 569-572.
Lind, O. and Kelber, A. (2009a). The intensity threshold of colour vision in two species of parrot. *J. Exp. Biol.* **212**, 3693-3699.
Lind, O. and Kelber, A. (2009b). Avian colour vision: effects of variation in receptor sensitivity and noise data on model predictions as compared to behavioural results. *Vision Res.* **49**, 1939-1947.
Lind, O. and Kelber, A. (2011). The spatial tuning of achromatic and chromatic vision in budgerigars. *J. Vision* **11**, 1-9.
Lind, O., Sunesson, T., Mitkus, M. and Kelber, A. (2012). Luminance-dependence of spatial vision in budgerigars (*Melopsittacus undulatus*) and Bourke's parrots (*Neopsephotus bourkii*). *J. Comp. Physiol. A* **198**, 69-77.
Lind, O., Chavez, J. and Kelber, A. (2014). The contribution of single and double cones to spectral sensitivity in budgerigars during changing light conditions. *J. Comp. Physiol. A* **200**, 197-207.
Lisney, T. J., Rubene, D., Rózsa, J., Løvlie, H., Håstad, O. and Ödeen, A. (2011). Behavioural assessment of flicker fusion frequency in chicken *Gallus gallus domesticus*. *Vision Res.* **51**, 1324-1332.
Osorio, D., Vorobyev, M. and Jones, C. D. (1999). Colour vision of domestic chicks. *J. Exp. Biol.* **202**, 2951-2959.
Osorio, D., Smith, A. C., Vorobyev, M. and Bucchanan-Smith, H. M. (2004). Detection of fruit and the selection of primate visual pigments for color vision. *Am. Nat.* **164**, 696-708.
Maier, E. J. (1992). Spectral sensitivities including the ultraviolet of the passeriform *Leiothrix lutea*. *J. Comp. Physiol. A* **170**, 709-714.
Maier, E. J. and Bowmaker, J. (1993). Colour vision in the passeriform bird, *Leiothrix lutea*: correlation of visual pigment absorbance and oil droplet transmission with spectral sensitivity. *J. Comp. Physiol. A* **172**, 295-301.
Prescott, N. B. and Wathes, C. M. (1999). Spectral sensitivity of the domestic fowl (*Gallus g. domesticus*). *Br. Poult. Sci.* **40**, 332-339.
Prins, N. and Kingdom, F. A. A. (2009). *Palamedes: Matlab Routines for Analysing Psychophysical Data*. Available at: http://www.palamedestoolbox.org.
Rieke, F. and Baylor, D. A. (1998). Single-photon detection by rod cells of the retina. *Rev. Mod. Phys.* **70**, 1027-1036.
Rieke, F. and Baylor, D. A. (2000). Origin and functional impact of dark noise in retinal cones. *Neuron* **26**, 181-186.
Rose, A. (1942). The relative sensitivities of television pickup tubes, photographic film, and the human eye. *Proc. Inst. Radio Eng.* **30**, 293-300.
Rose, A. (1948). The sensitivity performance of the human eye on an absolute scale. *J. Opt. Soc. Am.* **38**, 196-208.
Schaefer, H. M., Schaefer, V. and Vorobyev, M. (2007). Are fruit colors adapted to consumer vision and birds equally efficient in detecting colorful signals? *Am. Nat.* **169 Suppl. 1**, S159-S169.
Schnapf, J. L., Nunn, B. J., Meister, M. and Baylor, D. A. (1990). Visual transduction in cones of the monkey *Macaca fascicularis*. *J. Physiol.* **427**, 681-713.
Schmid, K. L. and Wildsoet, C. F. (1998). Assessment of visual acuity and contrast sensitivity in the chick using an optokinetic nystagmus paradigm. *Vision Res.* **38**, 2629-2634.
Schneeweis, D. M. and Schnapf, J. L. (1995). Photovoltage of rods and cones in the macaque retina. *Science* **268**, 1053-1056.
Vorobyev, M. (2003). Coloured oil droplets enhance colour discrimination. *Proc. Biol. Sci.* **270**, 1255-1261.

Vorobyev, M. and Osorio, D. (1998). Receptor noise as a determinant of colour thresholds. *Proc. Biol. Sci.* **265**, 351-358.
Vorobyev, M., Osorio, D., Bennett, A. T. D., Marshall, N. J. and Cuthill, I. C. (1998). Tetrachromacy, oil droplets and bird plumage colours. *J. Comp. Physiol. A* **183**, 621-633.
Vorobyev, M., Brandt, R., Peitsch, D., Laughlin, S. B. and Menzel, R. (2001). Colour thresholds and receptor noise: behaviour and physiology compared. *Vision Res.* **41**, 639-653.
Warrant, E. J. (1999). Seeing better at night: life style, eye design and the optimum strategy of spatial and temporal summation. *Vision Res.* **39**, 1611-1630.
Wyszecki, G. and Stiles, W. S. (2000). Visual thresholds. In *Color Science: Concepts and Methods, Quantitative Data and Formulae*, 2nd edn (ed. G. Wyszecki and W. S. Stiles), pp. 525-544. New York, NY: Wiley.
Yebra, A., Garcia, J. A., Nieves, J. L. and Romero, J. (2000). Chromatic discrimination in relation to luminance level. *Color Res. Appl.* **26**, 123-131.